

X-RAY MONITORING OF ULTRALUMINOUS X-RAY SOURCES

PHILIP KAARET¹ AND HUA FENG²
to appear in ApJ

ABSTRACT

X-ray monitoring observations were performed with the *Swift* observatory of the ultraluminous X-ray sources Holmberg IX X-1, NGC 5408 X-1, and NGC 4395 X-2 and also of the nuclear X-ray source in NGC 4395. Holmberg IX X-1 remains in the hard X-ray spectral state as its flux varies by a factor of 7 up to an (isotropic) luminosity of 2.8×10^{40} erg s⁻¹. This behavior may suggest an unusually massive compact object. We find excess power at periods near 60 days and 28 days in the X-ray emission from Holmberg IX X-1. Additional monitoring is required to test the significance of these signals. NGC 5408 X-1 and NGC 4395 X-2 appear to remain in the soft spectral state found by Chandra and XMM with little variation in spectral hardness even as the luminosity changes by a factor of 9. We found an outburst from the nuclear source in NGC 4395 reaching an X-ray luminosity of 9×10^{40} erg s⁻¹, several times higher than any previously reported.

Subject headings: black hole physics – galaxies: individual: Holmberg IX, NGC 5408, NGC 4395 – galaxies: stellar content – X-rays: galaxies – X-rays: black holes

1. INTRODUCTION

Ultraluminous X-ray sources (ULXs) were originally identified as potential intermediate-mass black holes (IMBHs) on the basis of the high luminosities inferred assuming isotropic emission of X-rays (Colbert & Mushotzky 1999; Makishima et al. 2000; Kaaret et al. 2001). If ULXs are, indeed, radiating isotropically below the Eddington luminosity, then the inferred masses are, in some cases, greater than $500M_{\odot}$. This is larger than the maximum compact object mass which can be formed in the collapse of a single star with metallicity $Z \gtrsim 10^{-3}Z_{\odot}$ (Bromm & Loeb 2003), and requires a different mechanism for formation. The existence of IMBHs would be of interest for subjects ranging from the formation of galaxies and their supermassive black holes to the generation of gravitational waves. However, the physical nature of ULXs is not well understood. The X-rays may be mechanically or relativistically beamed in which case IMBHs are not required.

New information is needed to understand the ULXs. Knowledge of the patterns of evolution of the X-ray emission from Galactic black hole X-ray binaries has been key to understanding their physical nature (Remillard & McClintock 2006; Belloni et al. 2005). Detailed study of spectral evolution was key to determining the physical nature of the spectral components contributing to the emitted X-ray flux.

Previously, it has been possible to obtain light curves with more than about a dozen points only for the brightest ULX located in M82 (Kaaret, Simet, & Lang 2006a,b; Kaaret & Feng 2007). The *Swift* observatory (Gehrels et al. 2004) has a capability, unique among focusing X-ray telescopes, to perform multiple observations of a given target with flexible scheduling. While the effective area of the Swift X-Ray Telescope (XRT) is limited in comparison with the larger X-ray observatories,

the brighter ULXs have sufficiently high fluxes to provide reasonable numbers of counts (~ 200) in modest individual observations (less than 2 ks). Thus, *Swift* provides the unique means to extend our knowledge of ULXs by probing their patterns of spectral evolution with dense temporal coverage.

Here, we report on X-ray monitoring observations performed with the *Swift* observatory of the ultraluminous X-ray sources Holmberg IX X-1, NGC 5408 X-1, and NGC 4395 X-2 and also of the nuclear X-ray source NGC 4395 X-1. The targets, observations, and data reduction are described in §2. The results are discussed in §3.

2. TARGETS, OBSERVATIONS, AND DATA ANALYSIS

Holmberg IX X-1 (= NGC 3031 X-9) has an average X-ray luminosity near 10^{40} erg s⁻¹ and is surrounded by a large and energetic optical nebula (Grisé et al. 2006). This ULX is one of the best on which to perform long term monitoring with *Swift* because it is the brightest ULX with no contaminating sources within the angular resolution of the Swift XRT. The source shows large flux variations across the observations obtained to date by various X-ray instruments (La Parola et al. 2001). Based on XMM-Newton spectra, we estimated a typical count rate for the Swift XRT of 0.14 c/s when retaining events with grades 0-12 in photon counting mode. Thus, measurement of the source intensity and a hardness ratio are possible with observations of around 1400 s. We obtained 72 observations of Holmberg IX X-1 under Swift program 90008 (PI Kaaret). In addition, we analyzed one observation obtained under program 25952, 9 from program 35335, and 25 from program 90079.

We also searched the *Swift* archive for series of multiple observations of other relatively bright ULXs. We found 78 observations of the ULX NGC 5408 X-1 under program 90041 and 24 under program 90218 (both PI Strohmayer). This ULX has exhibited quasiperiodic oscillations at relatively low frequencies (Strohmayer et al. 2007) and is surrounded by a powerful radio nebula (Kaaret et al. 2003; Soria et al. 2006; Lang et al. 2007) and a photoionized optical nebula (Kaaret & Corbel

¹ Department of Physics and Astronomy, University of Iowa, Van Allen Hall, Iowa City, IA 52242, USA

² Department of Engineering Physics and Center for Astrophysics, Tsinghua University, Beijing 100084, China

TABLE 1
SPECTRAL PARAMETERS OF ULXs

	Holm IX X-1	N5408 X-1	N4395 X-2
Hardness	0.80±0.01	0.43±0.01	0.35±0.02
χ^2/DoF	7.9/10	4.0/9	6.1/4
n_H (cm ⁻²)	2.0×10^{20}	1.4×10^{20}	2.4×10^{21}
Γ	1.88	3.06	4.12
Hardness	0.79	0.47	0.39

NOTE. — The table includes for each source: the average X-ray hardness measured with Swift, the column density and photon index measured from fits to XMM-Newton data of an absorbed power-law model, and the expected Swift hardness calculated using the XMM-Newton spectral fits.

2009). NGC 5408 X-1 is one of the best intermediate mass black hole candidates amongst the ULXs. However, NGC 5408 X-1 is dimmer than Holmberg IX X-1.

We also found 59 observations of the nearby active galaxy NGC 4395 obtained under program 90053 (PI Uttley). NGC 4395 contains an X-ray source at a position near RA = 12h26m02s, DEC 33d31'34" (J2000), NGC 4395 X-2 in Lira et al. (2000) and source E in Moran et al. (1999), that during the ROSAT-era appeared brighter than nuclear X-ray source, reaching a luminosity near 3×10^{39} erg s⁻¹. We examined this source. We also examined the nuclear X-ray source in NGC 4395, NGC 4395 X-1 in Lira et al. (2000) and source A in Moran et al. (1999), for comparison with the ULXs.

We retrieved level 2 event files with observations of these targets made in photon counting and pointed mode. These event files have data screening already applied as described in the XRT User's Guide. Each observation is divided up into one or more good time intervals (GTIs). We analyzed each GTIs separately, retaining only those GTIs with durations of 100 s or longer. We extracted source counts from a region with a radius of 25" and background counts from an annulus with an inner radius of 50" and an outer radius of 100". This extraction radius captures 82% of the total photon flux (Moretti et al. 2006) and we correct for this when calculating source fluxes. There are bad pixels in the XRT CCD that can lead to a loss of photons. For each GTI, we calculated the displacement of the center of gravity of the recorded photons from the nearest bad pixel and rejected the GTI if the displacement was less than 12.5". This removes GTIs that have one or more bad pixels near the core of the source point spread function. About 20% of the GTI were rejected due to bad pixels. Using the measured point spread function (Moretti et al. 2006) and making the conservative assumption that the nearest bad pixel is at the edge of a half-plane of bad pixels, we estimate that the maximum loss of counts for the unrejected GTIs is less than 6%. We performed our analysis using the Pulse Invariant (PI) data which are corrected for gain variations with time, temperature, and charge transfer inefficiency. For each observation interval, we calculated the net count rate in the 0.3-8 keV band and in the 1-8 keV band. We calculated a hardness ratio equal to the rate in the hard band (1-8 keV) divided by the rate in the full band (0.3-8 keV).

3. RESULTS

The X-ray light curves of the four targets in the 0.3-8 keV band are shown in Fig. 1. Significant variability is seen in all of the light curves. We calculated periodograms for the data shown in each light curve using the method of Horne & Baliunas (1986) with the power normalized by the total variance of the data for periods in the range of 4 to 130 days. The maximum power is 18.1 near a period of 115 days for NGC 5408 X-1 and 12.3 at a period near 28 days for NGC 4395 X-2; neither is a significant signal. The periodogram for Holmberg IX X-1 is shown in Fig. 2. There are two peaks: one with a power of 35.0 at a period near 60 days and one with a power of 31.6 at a period near 28 days. The fine structure of the peaks is due to aliasing of nearby periods due to the large gap in time between the different epochs of Swift observations. We note that a significant part of the power comes from the flare near MJD 54020 in observations taken before the start of the monitoring. Excluding the data from MJD 54000 to 54100, the strongest signal has a power of 23.1 at a period near 56 days. Thus, we do not interpret the signal as a true periodicity at this time. However, the observed signal is strong motivation to continue monitoring of Holmberg IX X-1 with *Swift*.

Hardness/intensity diagrams for the four targets are shown in Fig. 3. The intensity is the count rate in the 0.3-8 keV band and the hardness is the ratio of the rate in the hard band (1-8 keV) divided by the rate in the full band (0.3-8 keV). The individual good time intervals were generally too short to adequately constrain the hardness ratio, particularly for the dimmer sources. However, the hardness values for a given source at a given count rate appeared consistent. Thus, we chose to bin the data by count rate and calculate the average hardness for all of the observations within each count rate bin. The behavior of all three ULXs is consistent with no significant spectral evolution as a function of intensity. The average hardness and the χ^2 for a model where the hardness is taken as equal to the average are shown in Table 1. For comparison, we show the results of a fit of an absorbed power-law model to XMM-Newton data (Feng & Kaaret 2005) and the hardness that would be obtained observing such a spectrum with Swift. To estimate the sensitivity of the hardness ratio, we note that changing the photon index for Holmberg IX X-1 from 1.88 to 2.00 changed the hardness from 0.79 to 0.77. In all cases, the hardness calculated from the best fit XMM-Newton spectrum is in good agreement with the average hardness found from the Swift data. For Holmberg IX X-1, we separately examined the data with rates between 0.06 c/s and 0.3 c/s. The average hardness is 0.80 ± 0.01 and the goodness of fit for a constant model is $\chi^2/\text{DoF} = 5.8/7$. Thus, the data remain consistent with constant hardness even if the points with large errors are excluded.

Remillard & McClintock (2006) have identified three main spectral/timing states of accreting stellar-mass black holes: the steep power-law state, the thermal dominant state, and the hard state. The hard state is defined as having a photon index $1.4 < \Gamma < 2.1$. The Swift data show that Holmberg IX X-1 remains in the hard state, with Γ near 1.9, as the flux varies over a factor of ~ 7 . The highest counting rate observed with Swift corresponds to a flux of 1.8×10^{-11} erg cm⁻² s⁻¹ in the 0.3-10 keV band using the spectral model in Table 1 and a luminosity of 2.8×10^{40} erg s⁻¹ at the distance of 3.6 Mpc to Holmberg

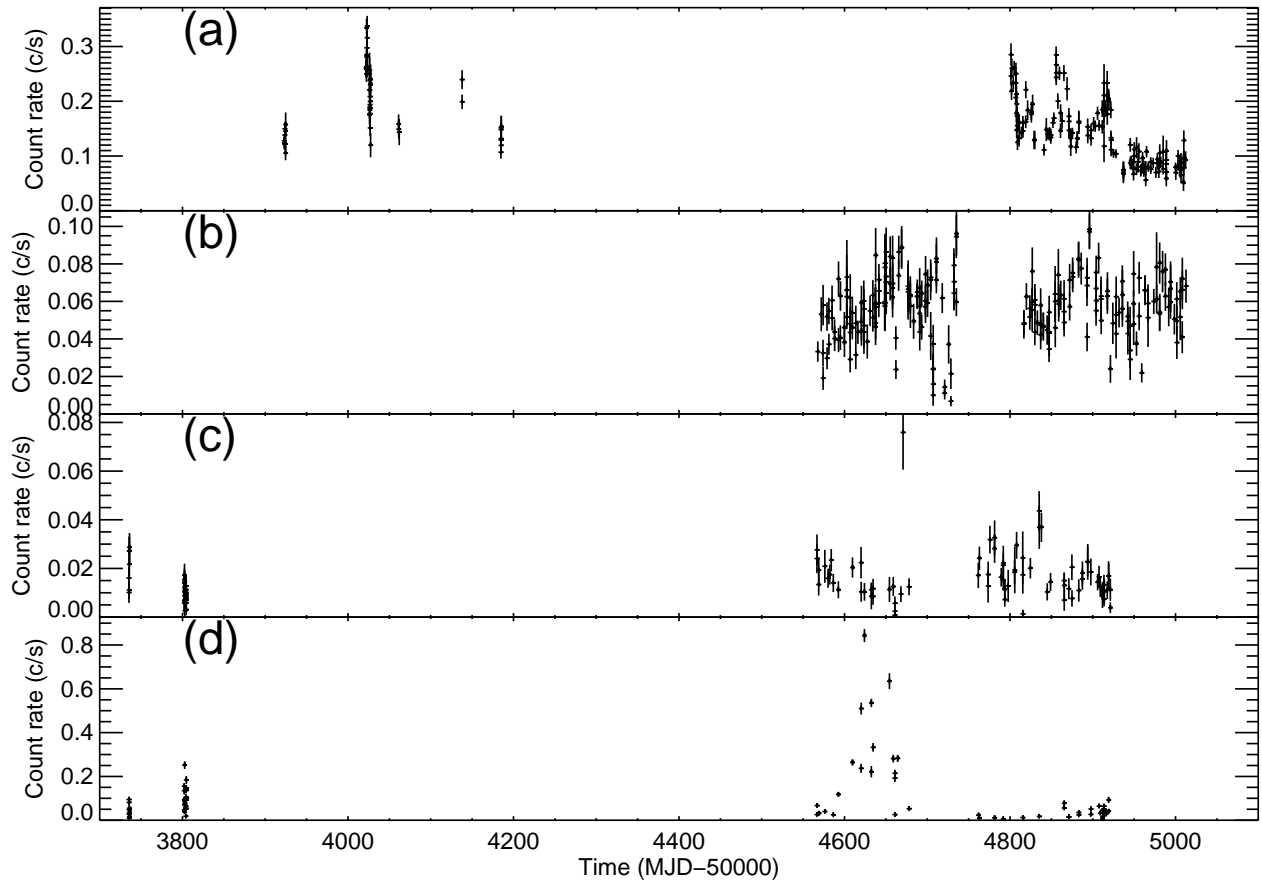


FIG. 1.— X-ray light curves in the 0.3-8 keV band for: (a) Holmberg IX X-1, (b) NGC 5408 X-1, (c) the ULX NGC 4395 X-2, (d) the nuclear source NGC 4395 X-1.

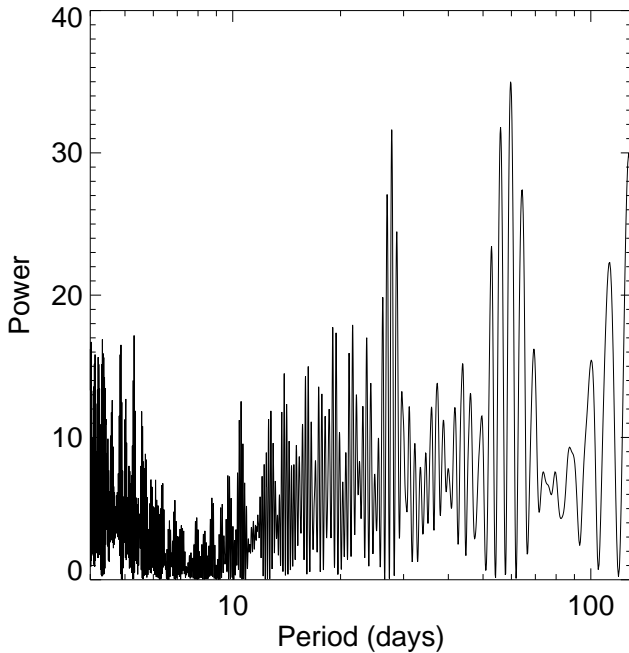


FIG. 2.— Periodogram calculated from the X-ray flux measurements of Holmberg IX X-1. Peak are apparent at a periods of 28.8 and 64.5 days.

IX assuming isotropic emission. Correcting for absorption increases this luminosity by 50%.

Stellar-mass black hole binaries can stay in the hard state for extended periods at luminosities below around

$0.05L_{\text{Edd}}$, where L_{Edd} is the Eddington luminosity. In particular, GX 339-4 has been observed to remain in the hard state for intervals of more than one year (Remillard & McClintock 2006; Miyakawa et al. 2008). Thus, the behavior observed from Holmberg IX X-1 may be similar to that observed from GX 339-4, but with a higher luminosity threshold for the transition out of the hard state implying a higher Eddington luminosity. If so, then an unusually massive black hole is required for Holmberg IX X-1. We note that some stellar-mass black holes have been observed in the hard state at luminosities as high as $0.3L_{\text{Edd}}$ (Rodriguez, Corbel, & Tomsick 2003; Zdziarski et al. 2004; Yuan et al. 2007; Miyakawa et al. 2008). However, such high hard-state luminosities are soon followed by a transition to a softer spectral state, which is not observed in Holmberg IX X-1.

The behavior of Holmberg IX X-1 is similar to that observed from a number of other particularly luminous ULXs that remain in the hard state even at the highest luminosities (Soria et al. 2007; Berghea et al. 2008; Kaaret et al. 2009; Soria et al. 2009; Feng & Kaaret 2009). These ULXs with hard spectra at luminosities above $10^{40} \text{ erg s}^{-1}$ are a particularly interesting class of objects and deserve further study.

The spectra of NGC 5408 X-1 and NGC 4395 X-2 are softer than found in the hard state. These sources appear to be in the steep power-law state, defined as a photon index $\Gamma > 2.4$. The Swift observations find these sources at luminosities $\lesssim 1 \times 10^{40} \text{ erg s}^{-1}$. There are several other ULXs that appear in the steep power-law state at similar

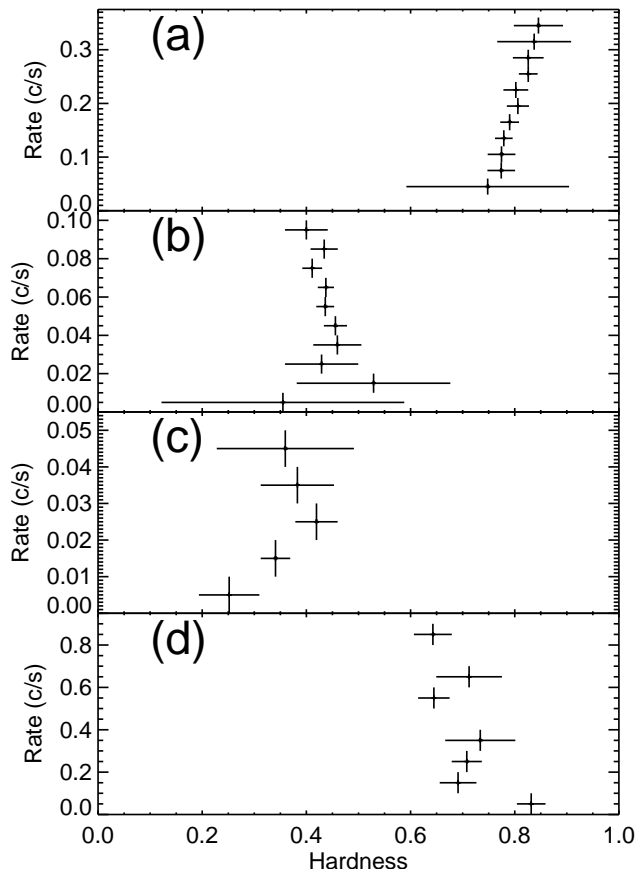


FIG. 3.— Hardness/intensity diagrams for the four sources: (a) Holmberg IX X-1, (b) NGC 5408 X-1, (c) the ULX NGC 4395 X-2, (d) the nuclear source NGC 4395 X-1.

luminosities (Feng & Kaaret 2005). The steep power-law state tends to occur at the highest luminosities seen from accreting stellar-mass black holes. These ULXs may represent a high luminosity extension of the steep power-law state.

NGC 4395 has been referred to as the least luminous type 1 Seyfert galaxy (Moran et al. 1999) due to measurements of very low luminosities with ROSAT. More recent observations covering a broader energy band suggest an average luminosity near 9×10^{39} ergs $^{-1}$ in the 0.5-10 keV band (Moran et al. 2005), within the range seen from ULXs. The light curve of the nucleus of NGC

4395 shows a strong flare near MJD 54624. We use a simple absorbed power-law model to convert the Swift count rates to fluxes. Following Moran et al. (1999), we adopt an absorption column density $N_H = 1.6 \times 10^{20}$ cm $^{-2}$. We use a photon index $\Gamma = 1.5$ which produces a hardness of 0.7, in reasonable agreement with the measured values. The true X-ray spectrum of NGC 4395 X-1 is more complex than this, but this approximation should be sufficient to produce rough flux estimates. The peak counting rate observed is 0.84 c/s and corresponds to a flux of 4.5×10^{-11} erg cm $^{-2}$ s $^{-1}$ in the 0.5-10 keV band and a luminosity of 9.1×10^{40} ergs $^{-1}$ at the distance of 4.1 Mpc. This is several times higher than any flux previously reported from NGC 4395 X-1.

The spectral evolution of the nuclear X-ray source in NGC 4395 is inconsistent with being constant. The χ^2/DoF for a model of constant hardness is 27.9/6 corresponding to a probability of occurrence of 1.0×10^{-4} . The spectrum appears to harden at the lowest flux levels observed. O’Neill et al. (2006) found a similar trend comparing two Chandra observations of NGC 4395 and suggested that the cause is variable absorption. NGC 4395 is known to exhibit dramatic long-term spectral variability on time scales of several years. Such dramatic variability is not apparent in the Swift data, but this may be because the Swift data cover only one year.

The monitoring programs described here demonstrate that Swift can be used to measure the flux and spectral evolution of ULXs and AGN on time scales of months to years. For the nuclear source in NGC 4395, the trend for harder spectra at lower fluxes seen in two Chandra observations (O’Neill et al. 2006) is confirmed with a sample of more than 100 observations and the highest X-ray luminosity ever seen, 9×10^{40} ergs $^{-1}$, was recorded. The three ULXs monitored do not show significant changes in spectral state over months to years. Two of the ULXs, NGC 5408 X-1 and NGC 4395 X-1, remain in a soft spectral state, equivalent to a photon index softer than 2.6, as their flux varies by factors of ~ 9 . The other ULX, Holmberg IX X-1, remains in a hard spectral state, equivalent to a photon index near 1.9, as its flux varies by a factor of 7 in observations spread over several years and with (isotropic) luminosities up to 2.8×10^{40} ergs $^{-1}$. This behavior may suggest an unusually massive compact object.

REFERENCES

- Belloni, T., Homan, J., Casella, P., van der Klis, M., Nespoli, E., Lewin, W.H.G., Miller, J.M., Mendez, M. 2005, *A&A*, 440, 207
 Bergheda, C.T., Weaver, K.A., Colbert, E.J.M., Roberts, T.P. 2008, *ApJ* to appear, arXiv:0807.1547
 Bromm, V. & Loeb, A. 2003, *Nature*, 425, 812
 Colbert, E.J.M. & Mushotzky, R.F. 1999, *ApJ*, 519, 89
 Feng, H. & Kaaret, P. 2005, *ApJ*, 633, 1052
 Feng, H., & Kaaret, P. 2009, *ApJ*, in press
 Gehrels, N. et al. 2004, *ApJ*, 611, 1005
 Grisé, F., Pakull, M.W., Motch, C. 2006, *IAUS*, 230, 302
 Horne, J.H. & Baliunas, S.L. 1986, *ApJ*, 302, 757
 Kaaret, P. et al. 2001, *MNRAS*, 321, L29
 Kaaret, P., Corbel, S., Prestwich, A.H., Zezas, A. 2003, *Science*, 299, 365.
 Kaaret, P., Simet, M.G., Lang, C.C. 2006, *Science*, 311, 491
 Kaaret, P., Simet, M.G., Lang, C.C. 2006, *ApJ*, 646, 174
 Kaaret, P. & Feng, H. 2007, *ApJ*, 669, 106
 Kaaret, P. & Corbel, S. 2009, *ApJ*, 697, 950
 Kaaret, P., Feng, H., Gorski, M. 2009, *ApJ*, 692, 653
 La Parola, V. et al. 2001, *ApJ*, 556, 47
 Lang, C.C., Kaaret, P., Corbel, S., Mercer, A. 2007, *ApJ*, 666, 79
 Lira, P., Lawrence, A., Johnson, R.A. 2000, *MNRAS*, 319, 17
 Makishima, K. et al. 2000, *ApJ*, 535, 632
 Miyakawa, T., Yamaoka, K., Homan, J., Saito, K., Dotani, T., Yoshida, A., Inoue, H. 2008, *PASJ*, 60, 637
 Moran, E.C. et al. 1999, *PASP*, 111, 801
 Moran, E.C. et al. 2005, *AJ*, 129, 2108
 Moretti, A. et al. 2006, *AIPC*, 836, 676
 O’Neill, P.M. et al. 2006, *ApJ*, 645, 160
 Remillard, R.A. & McClintock, J.E. 2006, *ARA&A*, 44, 49
 Rodriguez, J., Corbel, S., Tomsick, J.A. 2003, *ApJ*, 595, 1032
 Soria, R., Fender, R.P., Hannikainen, D.C., Read, A.M., & Stevens, I.R. 2006, *MNRAS*, 368, 1527
 Soria, R., Baldi, A., Risaliti, G., Fabbiano, G., King, A., La Parola, V., Zezas, A. 2007, *MNRAS*, 379, 1313

Soria, R., Risaliti, G., Elvis, M., Fabbiano, G., Bianchi, S.,
Kuncic, Z. 2009, ApJ, 695, 1614
Strohmayer, T. et al. 2007, ApJ, 660, 580
Yuan, F., Zdziarski, A. A., Xue, Y., Wu, X.-B. 2007, ApJ, 659,
541

Zdziarski, A. A., Gierliński, M., Mikołajewska, J., Wardziński, G.,
Smith, D.M., Harmon, B.A., Kitamoto, S. 2004, MNRAS, 351,
791